Measurements of Dynamic Scaling from Epitaxial Growth Front: Fe Film on Fe(001)

Y.-L. He, H.-N. Yang, T.-M. Lu, and G.-C. Wang
Department of Physics, Rensselaer Polytechnic Institute, Troy, New York 12180-3590
(Received 31 July 1992)

Dynamic scaling behavior has been observed during the growth of Fe films on Fe(001) using high-resolution low-energy electron diffraction technique. The interface width grows with time according to the power law $w \sim t^{\beta}$, with $\beta = 0.22 \pm 0.02$. Time-invariant self-affine behavior on the short-range scale has also been observed with the roughness exponent $\alpha = 0.79 \pm 0.05$. The time-invariant characteristic agrees with the recent prediction based on the dynamic scaling theory. From the measured growth exponents, we suggest that the growth of Fe film is more consistent with a conservative growth process.

PACS numbers: 64.60.Ht, 61.14.Hg, 68.55.Jk

The far-from-equilibrium dynamics of interface growth has attracted much attention in recent years. Theoretically, it is generally recognized that the surface morphology and dynamics of a growing interface exhibit simple dynamic scaling behavior despite the complication of the growth processes [1]. In thin-film growth, if nonlocal effects are negligibly small, the random fluctuation and the local smoothing effects (such as diffusion or side growth) will play key roles in the evolution of the surface morphology. The competition between fluctuation and smoothing eventually reaches a balance on a relatively short-range scale, so that the local surface morphology is statistically stationary (time-invariant) and self-affine. However, the competition does not reach a balance on a long-range scale. The global surface morphology thus proceeds to a steady growth with the evolution of vertical roughening and lateral coarsening. Two correlation lengths are assigned to describe the growth process: the mean surface height fluctuation w (called the interface width), which is a measure of the vertical roughness, and the lateral correlation length ξ, which characterizes the coarsening size. In the scaling regime, the roughening and coarsening grow with time according to power laws $w(t) \sim t^{\beta}$ and $\xi(t) \sim t^{\beta/\alpha}$. The exponent β is related to the growth process and α describes the surface "roughness." The generic dynamic scaling aspects of a complex growing interface can be represented by an equal-time height-height correlation function [1],

$$H(\mathbf{r},t) = \langle [h(\mathbf{r},t) - h(0,t)]^2 \rangle = 2[w(t)]^2 g\left(\frac{r}{\xi(t)}\right) = \begin{cases} 2(r/\eta)^{2\alpha}, & \text{for } r \ll \xi(t), \\ 2[w(t)]^2, & \text{for } r \gg \xi(t), \end{cases} \quad (1)$$

where $\mathbf{r} = (x,y)$ and $h(\mathbf{r},t) = z$ denote respectively the lateral and vertical coordinates of surface atomic positions. The scaling function $g(X) = 1$, for $X \gg 1$, provides a direct measure of the time-dependent interface width $w(t)$. As $X \ll 1$, $g(X) = X^{2\alpha}$ and this gives $H(\mathbf{r},t)$ a self-affine form in the short range. The time-invariant quantity $\eta = \xi w^{-1/\alpha}$ is interpreted physically as the average terrace size during crystalline growth. As reported previously, the short-range time-invariant characteristics, shown in Eq. (1), can lead to a time-invariant diffraction structure factor in reciprocal space [2].

The growth models can be classified in two types: the nonconservative and the conservative growth processes. In the nonconservative dynamics, as in the Eden model [3] or the ballistic deposition model [4], the side growth is allowed with the creation of voids and overhangs, but the relaxation mechanism such as desorption or diffusion is not dominant enough to eliminate these defects completely. This leads to a nonconservative volume growth as described by the Kardar, Parisi, and Zhang (KPZ) model [5]. For conservative growth [6], however, the primary relaxation mechanism is the surface diffusion. Since the desorption of atoms and formation of overhangs and voids are negligibly small, the mass and volume conservation laws play an important role in the growth. The growth exponents for one class of the conservative growth are $\alpha = \frac{2}{3}$ and $\beta = \frac{1}{5}$ for a $d = 2+1$ system [6]. The values may vary depending on the couplings with other effects. Early work [6] suggested that the molecular-beam-epitaxy process belongs to this category. However, recent studies [7] argued that it may not be the case and at least the long-time process is still governed by nonconservative KPZ dynamics.

Although extensive theoretical studies have predicted many important features in the epitaxial growth dynamics, very little experimental work has been performed to verify these predictions. In previous epitaxial growth experiments, either the short-range behavior (related to α) [8,9] or the time-dependent long-range feature (related to β) [10] was studied, but not both at the same time. Experiments designed to clarify issues in the growth dynamics which cover both the long-range and the short-range regimes during growth are still lacking so far. In this Letter, we report the experimental investigation of the dynamic growth from a crystalline epitaxial thin film using the high-resolution low-energy electron diffraction (HRLEED) technique [11]. The technique is very sensitive to both short-range and long-range interface morphology [2]. We are able to observe and measure quantitatively both the time-invariant and time-dependent scaling characteristics during the dynamic growth.

A buffer layer consisting of about 100 atomic layers of

Fe was first formed on the Au(001) surface to release the interface strain. The (00)-beam angular distribution of HRLEED intensity showed a very narrow profile sitting on a diffuse intensity profile at the Fe-Fe out-of-phase diffraction condition. At the in-phase diffraction condition, the diffuse intensity disappeared and the profile resembled the instrument response of the HRLEED system. We shall see later that this surface is basically flat and contains steps confined to only the top two layers of atoms. The interface width is negligibly small. The details of achieving such a buffer layer will be published elsewhere. We then began to study the dynamic scaling growth with a deposition rate ~ 2 monolayers/min. The surface morphology was characterized by HRLEED after every 3-min deposition interval. No significant self-annealing effect can be observed after a very long time after each Fe deposition. The diffraction line shapes remain the same even after one or two days.

The (00)-beam angular profiles of the HRLEED intensity were measured as a function of the incident electron beam energy E after each deposition. Figure 1(a) shows the line shapes of the (00)-beam intensity measured at different growth times at $E=40.0$ eV, corresponding to the Fe-Fe out-of-phase diffraction condition: $\phi \approx 3\pi$, where $\phi = k_\perp c$ (c is the vertical lattice spacing) and $k_\perp$ is the diffraction wave vector perpendicular to the surface. As shown in Fig. 1(a), the line shape at $t=0$ is basically a δ-like central spike (convoluted with the narrow instrument response) superimposed on a broad diffuse profile. As the film grows thicker and thicker, the central spike intensity quickly drops to zero. The decay of the δ component with time can also be shown at various diffraction conditions for different electron energies. Figure 2 is the peak-to-peak ratio (after decomposition of the profiles) of the δ intensity to the diffuse intensity measured as a function of $[\phi]$ at different times, where $[\phi]$ means ϕ modulo 2π such that $-\pi \le [\phi] \le \pi$. $[\phi]/\pi = 1$ is the out-of-phase condition and $[\phi]/\pi = 0.2$ is close to the in-phase condition ($[\phi]=0$).

The δ intensity is a measure of the long-range surface flatness. The continuous decrease of the δ intensity, as shown in Figs. 1 and 2, is a clear indication of the vertical roughening evolution. Such a growth-induced multilevel roughening can also be seen in the evolution of the energy-dependent diffuse intensity distribution. Figure 3 is the plot of the full width at half maximum (FWHM) of the diffuse line shape as a function of $[\phi]$ measured at different times. At $t=0$, the plot shows only a slight variation, implying that the surface fluctuation is confined nearly to the top two levels (the restricted two-level system [12] would give a constant curve of FWHM vs $[\phi]$). At $t>0$, as shown in Fig. 3, the growth leads to a significant variation (oscillation) of the FWHM as a

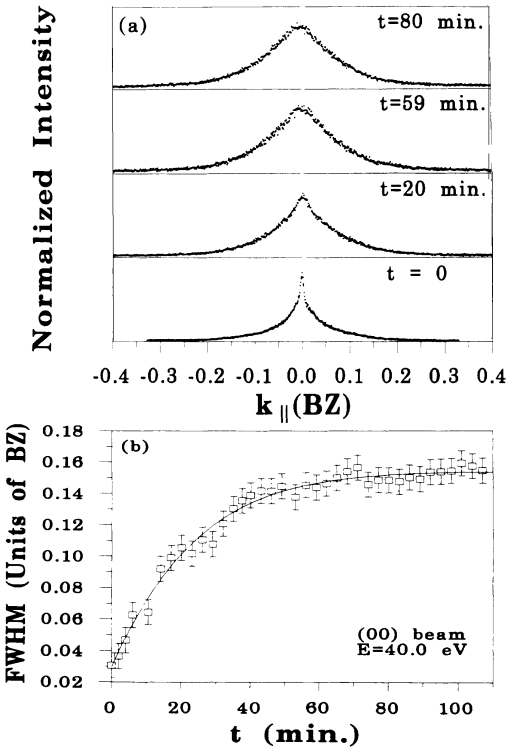

FIG. 1. (a) The angular profiles of the (00)-beam intensity measured at the out-of-phase diffraction condition, $\phi \approx 3\pi$, at different times during growth. (b) The corresponding FWHM as a function of time, where the solid curve is a guide to the eyes. At $t=0$ shown in (a), the central part of the line shape has a Gaussian-like portion (the δ component of the line shape discussed in the text) with a narrow width equal to the instrument response of HRLEED. For Fe(001), the size of the Brillouin zone (BZ) is 2.19 Å^{-1}.

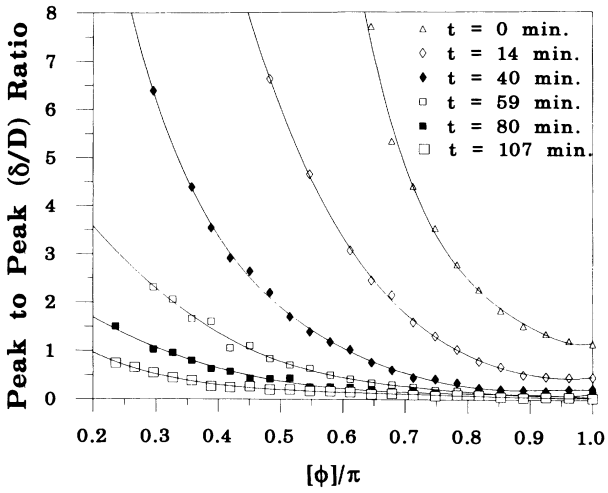

FIG. 2. After the decomposition of the central peak and the diffuse line shape, the peak-to-peak ratio of the δ intensity to the diffuse intensity is plotted as a function of the diffraction condition $[\phi]$ at different times during growth. The ratio should have a minimum value at the out-of-phase condition, $[\phi] \sim \pi$, due to the destructive interference of the wave diffracted from a stepped surface. The solid curves are guidelines through data points with uncertainties $\sim \pm 10\%$.

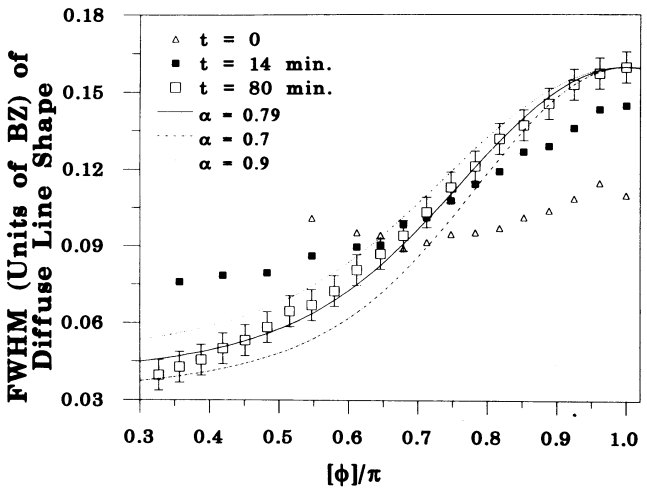

FIG. 3. The FWHM of the diffuse line shape plotted against $[\phi]$ at different times during growth. The oscillation of the FWHM indicates the existence of the multilevel step surface. The solid curve is the fit of the experimental data (open squares) taken at $t=80$ min, corresponding to $\alpha=0.79$. To show the sensitivity of the fit, we also plot two dashed curves near the solid curve, which correspond to $\alpha=0.7$ and 0.9.

function of $[\phi]$ and, therefore, the formation of a multilevel step structure. At the in-phase diffraction condition, the electron wave is not sensitive to surface steps and the profiles remain sharp (instrument response) at all times during growth.

In contrast to the time-dependent evolution shown above, at the out-of-phase condition, where the δ intensity quickly decays to zero, the diffraction is not sensitive to the long-range change during growth. As shown at 59 and 80 min in Fig. 1(a), the residual diffuse angular profiles do not undergo any further change after the disappearance of the δ component. Such a time-invariant behavior can be demonstrated more clearly in Fig. 1(b) where the FWHM of the entire angular profile at the out-of-phase condition is plotted as a function of time. After the gradual increase due to the initial roughening evolution, as shown in the first 40 min, the entire profile remains stationary and the FWHM reaches a constant value for $t>40$ min. (At $t=107$ min, about 214 atomic layers of Fe have been grown starting from $t=0$.) Our measurements confirm the existence of the short-range time-invariant characteristic as predicted recently according to the dynamic scaling theory [2]. The observed time-invariant behavior at this diffraction condition is therefore an indication of the fact that the system has already reached a dynamic scaling regime.

The interface width w can be measured based on the well-developed kinematic diffraction theory. The diffraction intensity $I(\mathbf{k}_\parallel,k_\perp,t)$ represents the Fourier transform of the "height difference function,"

$$C_\phi(\mathbf{r},t)=\langle\exp\{i\phi[h(\mathbf{r},t)-h(0,t)]\}\rangle,$$

i.e.,

$$I(\mathbf{k}_\parallel,k_\perp,t)=\int d^2r\,e^{i\mathbf{k}_\parallel\cdot\mathbf{r}}C_\phi(\mathbf{r},t)$$
$$=(2\pi)^2C_\phi(\mathbf{r}\to\infty,t)\delta(\mathbf{k}_\parallel)+I_{\rm diff}(\mathbf{k}_\parallel,k_\perp,t), \quad (2)$$

where $\mathbf{k}_\parallel$ is the wave vector parallel to surface. The last step in Eq. (2) reexpresses the intensity as a sum of a δ component and a diffuse intensity function given by

$$I_{\rm diff}(\mathbf{k}_\parallel,k_\perp,t)=\int d^2r\,e^{i\mathbf{k}_\parallel\cdot\mathbf{r}}[C_\phi(\mathbf{r},t)-C_\phi(\mathbf{r}\to\infty,t)]. \quad (3)$$

An intrinsic connection of $C_\phi(\mathbf{r},t)$ to the height-height correlation $H(\mathbf{r},t)$ has been obtained according to the Gaussian approximation [13]

$$C_\phi(\mathbf{r},t)=\frac{\sum_{m=-\infty}^{m=+\infty}e^{-(1/2)H(\mathbf{r},t)(\phi-2\pi m)^2}}{\sum_{m=-\infty}^{m=+\infty}e^{-(1/2)H(\mathbf{r},t)(2\pi m)^2}}, \quad (4)$$

where the lowest order is $C_\phi(\mathbf{r},t)\sim e^{-(1/2)H(\mathbf{r},t)[\phi]^2}$. The higher-order terms result from the discrete lattice effect, which cannot be ignored at the near out-of-phase condition [2,14].

The coefficient of the δ intensity, $C_\phi(\mathbf{r}\to\infty,t)\sim e^{-w(t)^2[\phi]^2}$, is a measure of the long-range ($r\to\infty$) properties in the growing interface and is very sensitive to the interface width $w(t)$. Besides, $C_\phi(\mathbf{r}\to\infty,t)$ is also sensitive to the diffraction condition $[\phi]$. The decay of the δ intensity should be much quicker when $[\phi]$ is close to the out-of-phase condition. All these aspects are clearly observed in our measurements shown in Figs. 1 and 2. To obtain w, we measure the integrated intensities for both the δ component and the diffuse profile. According to Eq. (2), the integrated intensities have a simple relation,

$$R=\frac{\int d^2k_\parallel I_\delta(\mathbf{k}_\parallel,k_\perp,t)}{\int d^2k_\parallel I(\mathbf{k}_\parallel,k_\perp,t)}=C_\phi(\mathbf{r}\to\infty)\approx e^{-w(t)^2[\phi]^2}, \quad (5)$$

where $I_\delta(\mathbf{k}_\parallel,k_\perp,t)=(2\pi)^2C_\phi(\mathbf{r}\to\infty,t)\delta(\mathbf{k}_\parallel)$. In Fig. 4, we plot $\ln R$ (natural logarithm of the ratio R of integrated δ intensity to the total integrated intensity) as a function of $[\phi]^2$. The integration is over 50% of the 2D Brillouin zone. All the plots at different times t exhibit linear relations, which are consistent with Eq. (5). The plot of $\ln R$ vs $([\phi]/\pi)^2$ should give a slope equal to $-[\pi w(t)]^2$. The systematic increase of the slope with time in Fig. 4 is therefore another indication of the growth-induced roughening evolution. Shown as an inset in Fig. 4 is the measured slope versus time on a log-log plot. The log-log plot seemingly demonstrates a linear relation, which gives a power-law form, $[w(t)]^2\propto t^{2\beta}$. The growth exponent β can then be extracted and is found to be $\beta=0.22\pm0.02$.

The short-range self-affine property of the growing interface can be further examined from the diffuse intensity distribution measured at different diffraction conditions. The diffuse line shape can be fitted with the formula given by Eqs. (1), (3), and (4), where one can use a phe-

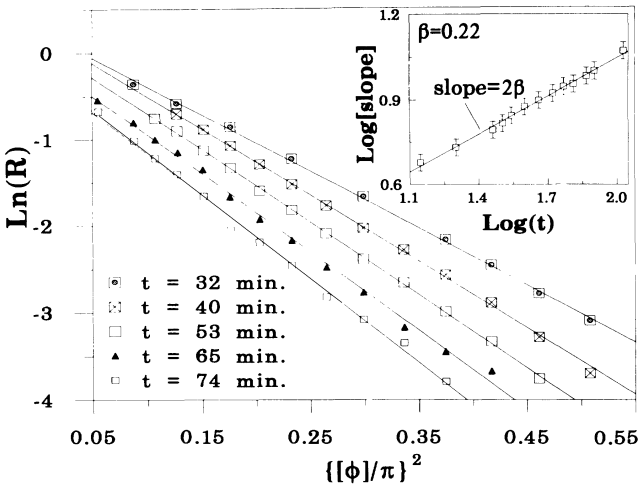

FIG. 4. $\ln R$ plotted as a function of $\{[\phi]/\pi\}^2$ at different times during growth. The plot should give a slope $-[\pi w(t)]^2$, according to Eq. (5). The measured slope vs time is then plotted in the inset on a log-log scale. The linear relation shown in the inset indicates that the interface width grows in the form of a power law, $[w(t)]^2 \propto t^{2\beta}$, with $\beta = 0.22$.

nomenological scaling function [15], $g(X) = 1 - e^{-X^{2\alpha}}$. We found that the diffuse line shape of I_{diff} vs $\mathbf{k}_\parallel$ is not very sensitive to the value of α (it can be fitted with a range of α from 0.5 to 1.0). However, we found that the variation of the FWHM vs $[\phi]$, where $\phi = k_\perp c$, is quite sensitive to α. We perform the fit from the out-of-phase regime to the time-dependent regime up to $[\phi] \sim 0.3\pi$. During the fit, α and η are the adjustable parameters while the time-dependent w is treated as a known parameter that varies from 0.8 to 1.1 as obtained from Fig. 4. It is found that the shape of the FWHM versus $[\phi]$ plot depends only on α and the magnitude of the FWHM depends on the value of η. The solid curve in Fig. 3 shows the best fit for the experimental data, which gives $\alpha = 0.79 \pm 0.05$ and $\eta = 14.0 \pm 2.0$ Å.

Our present experiment suggests that the deposition of Fe on Fe(001) belongs to a conservative growth process. The overhangs and voids are unlikely to appear in the growth of metal thin films not only because the surface diffusion plays a dominant role but also because metal atoms lack local chemical bonding such as dangling bonds. Most recent experiments that characterize self-affine fractals using different techniques [8] indicate that the values of α measured from metal thin films range from 0.65 to 0.95, which are indeed higher than that predicted by the nonconservative growth models [3–5] where a suggested value is $\alpha \sim 0.5$. The exponents, $\alpha = 0.79 \pm 0.05$ and $\beta = 0.22 \pm 0.02$, obtained in the present experiment, are thus more consistent with the results of conservative growth models [6]. Our result is also consistent with the recent experiment of Fe/Si(111) growth [10], where β was obtained to be ~ 0.25.

In conclusion, the dynamic scaling growth process has been realized in an epitaxial system, Fe/Fe(001). We have observed both the time-invariant and time-dependent characteristics during growth. The dynamic scaling law given by Eq. (1) has been examined from a short range of a few atomic distances to a long range of ~ 1000 Å (limited by the resolution of HRLEED). Our quantitative measurements of the growth exponents suggest that the growth of this metal thin film is more consistent with a conservative growth process.

This work is supported by NSF under Grant No. 8906003 and by ONR under Grant No. N00014-91-J-1099.

[1] For a review, see F. Family, Physica (Amsterdam) **168A**, 561 (1990); for recent reviews, see *Solids Far From Equilibrium: Growth Morphology and Defects*, edited by C. Godriche (Cambridge Univ. Press, New York, 1991), pp. 432 and 479.

[2] H.-N. Yang, T.-M. Lu, and G.-C. Wang, Phys. Rev. Lett. **68**, 2612 (1992).

[3] R. Jullien and R. Botet, J. Phys. A **18**, 2279 (1985); J. G. Zabolitzky and D. Stauffer, Phys. Rev. Lett. **57**, 1809 (1986); J. Kertész and D. E. Wolf, J. Phys. A **21**, 747 (1988); D. E. Wolf and J. Kertész, Europhys. Lett. **4**, 651 (1987).

[4] M. J. Vold, J. Colloid Sci. **14**, 168 (1959); F. Family and T. Vicsek, J. Phys. A **18**, L75 (1985).

[5] M. Kardar, G. Parisi, and Y. Zhang, Phys. Rev. Lett. **56**, 889 (1986).

[6] J. Villain, J. Phys. I (France) **1**, 19 (1991); D. E. Wolf and J. Villain, Europhys. Lett. **13**, 389 (1990); Z.-W. Lai and S. Das Sarma, Phys. Rev. Lett. **66**, 2348 (1991); L.-H. Tang and T. Nattermann, Phys. Rev. Lett. **66**, 2899 (1991).

[7] Hong Yan, Phys. Rev. Lett. **68**, 3048 (1992); D. A. Kessler, H. Levine, and L. Sander, Phys. Rev. Lett. **69**, 100 (1992).

[8] R. Chiarello, V. Panella, J. Krim, and C. Thompson, Phys. Rev. Lett. **67**, 3408 (1991), and references therein; M. W. Mitchell and A. Bonnell, J. Mater. Res. **5**, 2244 (1990); J. M. Gómez-Rodriguez, A. M. Baró, and R. C. Salarezza, J. Vac. Sci. Technol. B **9**, 495 (1991).

[9] Y.-N. Yang, Y.-S. Luo, and J. H. Weaver, Bull. Am. Phys. Soc. **37**, 666 (1992).

[10] J. Chevrier, V. Le Thanh, R. Buys, and J. Derrien, Europhys. Lett. **16**, 737 (1991).

[11] U. Scheithauer, G. Meyer, and M. Henzler, Surf. Sci. **178**, 441 (1986); J.-K. Zuo, R. A. Harper, and G.-C. Wang, Appl. Phys. Lett. **51**, 250 (1987).

[12] For $d = 2+1$, see H.-N. Yang, K. Fang, G.-C. Wang, and T.-M. Lu, Europhys. Lett. **19**, 215 (1992); for $d = 1+1$, see C. S. Lent and P. I. Cohen, Surf. Sci. **139**, 121 (1984); J. M. Pimbley and T.-M. Lu, J. Vac. Sci. Technol. A **2**, 457 (1984); J. Appl. Phys. **57**, 1121 (1985).

[13] J. Villain, D. R. Grempel, and J. Lapujoulade, J. Phys. F **15**, 809 (1985).

[14] H.-N. Yang, T.-M. Lu, and G.-C. Wang (to be published).

[15] S. K. Sinha, E. B. Sirota, S. Garoff, and H. B. Stanley, Phys. Rev. B **38**, 2297 (1988).